

# RSEND: Retinex-based Squeeze and Excitation Network with Dark Region Detection for Efficient Low Light Image Enhancement

Jingcheng Li<sup>✉</sup>, Ye Qiao<sup>✉</sup>, Haocheng Xu<sup>✉</sup>, and Sitao Huang<sup>✉</sup>

University of California, Irvine CA 92697, USA

**Abstract.** Images captured under low-light scenarios often suffer from low quality. Previous CNN-based deep learning methods often involve using Retinex theory. Nevertheless, most of them cannot perform well in more complicated datasets like LOL-v2 while consuming too much computational resources. Besides, some of these methods require sophisticated training at different stages, making the procedure even more time-consuming and tedious. In this paper, we propose a more accurate, concise, and one-stage Retinex theory based framework, RSEND. RSEND first divides the low-light image into the illumination map and reflectance map, then captures the important details in the illumination map and performs light enhancement. After this step, it refines the enhanced gray-scale image and does element-wise matrix multiplication with the reflectance map. By denoising the output it has from the previous step, it obtains the final result. In all the steps, RSEND utilizes Squeeze and Excitation network to better capture the details. Comprehensive quantitative and qualitative experiments show that our Efficient Retinex model significantly outperforms other CNN-based models, achieving a PSNR improvement ranging from 0.44 dB to 4.2 dB in different datasets and even outperforms transformer-based models in the LOL-v2-real dataset.

**Keywords:** low light image enhancement · Squeeze and excitation network · compact model

## 1 Introduction

Low-light image enhancement aims to improve the visibility and perceptual quality of images captured in underexposed environments. This field addresses challenges such as noise, color distortion, and loss of detail, which commonly affect low-light images.

A large number of approaches have been proposed for low-light image enhancement. Traditional image enhancement methods mainly include Retinex theory-based algorithm and histogram equalization. However, histogram equalization sometimes leads to over-amplification of noise in relatively dark areas of an image as well as a loss of detail in brighter sections. This technique applies a global adjustment to the image’s contrast, which may not be suitable for

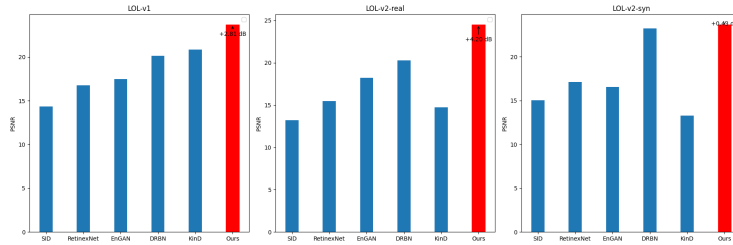


**Fig. 1:** Comparison of our RSEND against previous CNN based state-of-the-art methods including SID [3], RetinexNet [21], EnGAN [12], DRBN [24], KinD [29] on three datasets. Our method shows a marked improvement, as indicated by the red bars and the associated increase annotated above them.

images where local contrast variations are important for detail visibility. As for Retinex theory-based methods, they assume an image could be decomposed into illumination and reflectance, while preserving the reflectance, by only enhancing the illumination can they get the final enhanced image. However, such methods sometimes produce results that appear unnatural due to over-enhancement or incorrect color restoration. Additionally, these models might struggle with very dark regions where information is minimal, potentially leading to artifacts or noise amplification.

With the advancement of deep learning, Convolutional Neural Networks (CNNs) have become a pivotal technology for enhancing images captured in low-light conditions. Various types of CNN architectures have been explored, mainly they are divided into two categories, Generative Adversarial Networks (GANs) and models inspired by Retinex theory. For GANs, the adversarial process helps improve the quality of the enhancement, making images look more natural while suffering from training instability, leading to artifacts or unrealistic results, especially under complex lighting conditions. As for Retinex theory-based deep learning models, they typically decompose an image into reflectance and illumination components. The models estimate these components separately, enhancing the illumination part to improve image visibility while preserving the reflectance to maintain color fidelity and details. One drawback of such models is their reliance on accurate decomposition, which can be challenging in complex lighting conditions, and they always suffer from the multi-stage training pipeline.

Another problem is that previous methods always consume a large number of parameters, and heavy computational complexity is unaffordable in certain situations. For example, privacy concerns are paramount when processing sensitive images on local devices. If we have a compact and efficient network, we can ensure that data processing occurs on the device itself, especially for mobile applications where memory and processing power are limited. And when deploying models in the cloud, reducing cost is a critical factor. Smaller models require less computational power, thereby saving more energy and reducing the financial burden associated with cloud resources.

To fix the aforementioned problems, we propose a novel method, RSEND, to deal with low-light image enhancement tasks. First, we follow the Retinex theory methodology, decomposing the image into the illumination map and reflectance map. We add a dark region detection module so that the illumination map can further go through a multi-scale, separate pathway before enhancing to locate the features that need to be enhanced. Then we go through our U-shape [19] enhancer, and refine our image for better details. After the enhanced grayscale image does element-wise multiplication with the reflectance map, we add the original image to maintain similarity. And finally, we denoise the output for a more visually pleasing result. By utilizing Squeeze-and-Excitation Blocks [10] in all the steps mentioned, the network can recalibrate channel-wise feature responses by explicitly modeling inter-dependencies between channels, capturing more image details while not increasing substantial computational cost. We will open source this work to facilitate future research. Link to the source code can be found in the supplementary materials.

Our contributions are summarized as follows:

- We propose RSEND, a one-stage Retinex-based network, for efficient low-light image enhancement with light computation and high accuracy, free from tedious multi-stage training, and maintains good performance.
- Our method leverages squeeze and excitation network [10] to significantly enhance the representational power of the network, we largely make our network perform better without a substantial increase in computational complexity.
- We use a residual learning way in the reconstruction step to make sure our output is similar to the original low-light image, maintaining high SSIM.
- Our model outperforms all other CNN-based low-light image enhancement networks and even transformer-based models while costing much fewer computational resources.

## 2 Related Work

### 2.1 Traditional Methods

Traditional methods for low-light image enhancement, such as histogram equalization [11] [4] and gamma correction [7], focus on globally adjusting image contrasts or brightness. While these methods are simple and fast, they often overlook local context and can lead to unrealistic effects or artifacts, such as over-enhancement, under-enhancement in certain areas, or amplified noise. These limitations stem from their global processing nature, which does not account for local variations in light distribution within an image. As a result, while effective for moderate adjustments, they may struggle with images having complex light conditions or requiring nuanced enhancements.

## 2.2 Deep learning Methods

With the fast development of deep learning, CNNs [24], [3], [29], [6] have been extensively used in low light image enhancement. EnlightenGAN [12] utilizes unsupervised learning for low-light image enhancement, leveraging a global-local discriminator structure to ensure detailed enhancement and incorporates attention mechanisms to refine areas needing illumination adjustment, but a potential drawback is the challenge of maintaining naturalness and avoiding over-enhancement, especially in images with highly variable light conditions. ZeroDCE [8] tackles low-light image enhancement through a novel deep curve estimation approach that dynamically adjusts the light enhancement of images without needing paired datasets, which introduces a lightweight deep network to learn enhancement curves directly from data. However, like many approaches using unpaired datasets, its performance may depend on the diversity and quality of the training data, potentially limiting its adaptability to unseen low-light conditions. Retinex-based deep learning models [21] focus on separating the illumination and reflectance components of an image, allowing for the manipulation of illumination while preserving the natural appearance of the scene. Nevertheless, these networks always suffer from multi-stage training pipelines and face challenges including maintaining color fidelity and avoiding artifacts.

## 2.3 Squeeze-and-Excitation Network

The Squeeze-and-Excitation Network (SENet) [10] introduces a mechanism to recalibrate channel-wise feature responses adaptively by explicitly modeling interdependencies between channels. It squeezes global spatial information into a channel descriptor using global average pooling, then captures channel-wise dependencies through a simple gating mechanism, and finally excites the original feature map by reweighting the channels. The SENet approach has been applied to a wide range of tasks beyond low-light image enhancement, such as image classification, object detection, semantic segmentation, and medical image analysis. It has also been used in this area, The Multiscale Low-Light Image Enhancement Network with Illumination Constraint [6] utilizes SENet for low-light image enhancement. However, it consumes substantial computational resources for training and inference while not reaching a desired PSNR value.

## 3 RSEND: Efficient Low-Light Image Enhancement

In this section, we introduce our method RSEND, as shown in Fig. 2. We then provide the details of our work.

### 3.1 End-to-end Retinex-based Model

As we mentioned previously, Retinex theory has been extensively used in this area, A low light image  $S \in \mathbb{R}^{H \times W \times 3}$  can be decomposed into reflectance  $R \in$

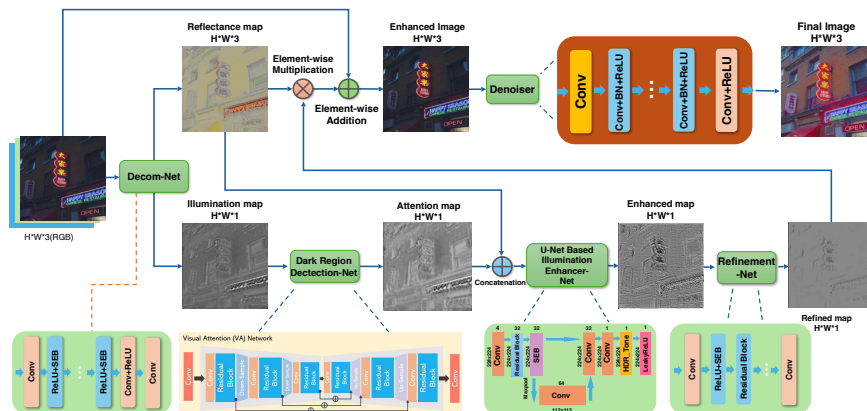


**Fig. 2:** The proposed framework of RSEND. Our network consists of five subnets: a Decom-Net, a Dark Region Detection-Net, an Enhancer-Net, a Refinement-Net, and a Denoiser. The Decom-Net decomposes the low-light image into a reflectance map and an illumination map based on the Retinex theory. The Dark Region Detection-Net means to find the regions that need to be enhanced more. The Enhancer-Net functions to illuminate the illumination map. The Refinement-Net aims to adjust contrasts and fine-tune the details. In the end, Denoiser performs denoising to get clean and visually pleasing output.

$\mathbb{R}^{H \times W \times 3}$  and illumination  $I \in \mathbb{R}^{H \times W}$

$$S = R \circ I, \quad (1)$$

the  $\circ$  here represents element-wise multiplication. Similar to the previous approaches, we decompose the image into reflectance and illumination that is designed to enhance. Unlike RetinexNet [21] to manually separate the first three channels as  $R$  and last channel as  $I$  after a few convolutional layers, we are inspired by Retinexformer [2] and like many other models did, after feature extraction, use two different layers in the end, one outputs three channels and the other outputs one channel, to separate  $R$  and  $I$  and use SEBlock in the middle for better feature extraction.

### 3.2 The Illumination Procedure

Instead of directly enhancing the illumination map, we add a few more illumination constraints. Before enhancing, we design a dark region detection module, using convolutions at Illumination map with kernel 3x3 and 5x5 and stride set as 2 to capture features at different scales, then apply sigmoid activation to generate attention maps, which weights the importance of each region needs to be enhanced. By upsampling the features from different scales to the original size

and doing concatenation with the original feature map, we come up with a feature map that has channels\*3 depth and features from both attention-augmented pathways. In the end, we apply a 1x1 kernel size convolutional layer to the concatenated multi-scale features to reduce the channel dimensions to  $I \in \mathbb{R}^{H \times W \times 1}$ . By applying this module, the network is expected to pay more attention to the darker areas that need enhancement.

$$\hat{I} = D(I), \quad (2)$$

As we illustrated in Fig. 2, our illumination enhancer is a type of U-Net [19] architecture. The input of this enhancer is the pre-processed illumination map concatenated with reflectance, which gives the enhancer more details about the image’s lighting and color information to consider besides the gray-scale image. For encoder, after applying convolutions to increase the channel depth to 32, we apply residual block to prevent vanishing gradient and SEBlock for modeling inter-dependencies between channels. In the bottleneck, our depth increases to 64 for capturing more complex features, and in our case, a depth of 64 is enough. As for the decoder path, the skip connections between the encoder and decoder blocks allow for the combination of high-level features. In the final layer, we apply high dynamic range (HDR) [5] and tone mapping [17], processing the feature maps from the decoder path to produce the final output image that has enhanced details in both the bright and dark areas.

$$\bar{I} = E(\hat{I}, R), \quad (3)$$

After enhancement, we have a layer for refinement, which aims to fine-tune the details, adjust contrasts, and improve overall image quality. The network designed here is simpler, the core of this layer is made of convolutional layers with a kernel size of 3 and padding of 1, and like previous parts, we implement residual blocks and SEBlocks for better performance.

### 3.3 Reconstruction and Denoising Phase

As mentioned previously, after we obtain the enhanced  $I$ , we perform element-wise multiplication with  $R$ . However, unlike the Retinex theory, we add the original low-light image to the product, which serves as a form of residual learning [9], helping to retain the structure and details from the original image while adjusting the illumination.

$$\bar{S} = \bar{I} \circ R + S, \quad (4)$$

Even though Retinex theory successfully enhances a low-light image, the process of enhancing can introduce or amplify noise. This is because when you increase the brightness of the dark regions, where the signal-to-noise ratio is usually lower, you also make the noise more visible. So after reconstruction, we also add a denoising phase, ensuring that the final output image is not only well-illuminated but also clean and visually pleasing. It’s important to note that for real-world images, especially those taken in low-light conditions, are likely to contain noise.

Thus, denoising is a crucial step in the image enhancement pipeline. Our denoising architecture is inspired by DnCNN [28], it is constructed as a sequence of convolutional layers, batch normalization layers, activation functions, SEBlocks, and residual blocks. In the forward method, residual learning is applied, and the input is added back to the output of the network, ensuring that the denoised image maintains structural similarity to the original. The final formula can be formulated as

$$\bar{S} = \epsilon(E(D(I), R) \circ R + S). \quad (5)$$

### 3.4 Compact Network

For low-light image enhancement tasks, previous CNN-based models always add layers and increase depth for more feature representation. However, this usually does not yield promising results while largely increasing computational costs. Our RSEND framework exemplifies the principle of reducing computational costs by integrating key design choices that promote efficiency. Firstly, the use of Squeeze-and-Excitation blocks allows the model to perform dynamic channel-wise feature recalibration, which significantly boosts the representational power of the network without a proportional increase in parameters. Secondly, we carefully design the depth of the network so that each layer contributes meaningfully to the feature extraction process. Previous works always reach a depth of 512 in the bottleneck of the enhancer, while in our work, the bottleneck only has 64 channels and in other modules of the network the depth is restrained to 32. The result in Table 1 shows that it is possible to build powerful yet compact models with a fraction of the parameters in the realm of low-light image enhancement.

### 3.5 Loss Function

Our training objective consists of several loss components designed to capture different aspects of image quality in low-light image enhancement tasks. Each term contributes to a specific characteristic that we aim to imbue in the enhanced output.

**Spatial Consistency Loss** The Spatial Consistency Loss  $\mathcal{L}_{spa}$  enhances the spatial coherence of the enhanced image by maintaining the difference of neighboring regions between the input and its enhanced version:

$$\mathcal{L}_{spa} = \frac{1}{K} \sum_{i=1}^K \sum_{j \in \Omega(i)} (|Y_i - Y_j| - |I_i - I_j|)^2, \quad (6)$$

where  $K$  represents the number of local regions,  $\Omega(i)$  denotes the four neighboring regions (top, down, left, right) centered at region  $i$ .  $Y$  and  $I$  are the average intensity values of the local region in the enhanced and input images, respectively.

**Exposure Control Loss** The Exposure Control Loss  $\mathcal{L}_{exp}$  aims to correct under-/over-exposed regions by controlling the exposure level. It measures the distance between the average intensity of a local region and a predefined well-exposedness level  $E$ :

$$\mathcal{L}_{exp} = \frac{1}{M} \sum_{k=1}^M |Y_k - E|, \quad (7)$$

where  $M$  is the number of non-overlapping local regions,  $Y_k$  is the average intensity value of the  $k^{th}$  local region in the enhanced image, and  $E$  is the target exposure level. In our case, we set  $E$  as 0.6.

**Color Constancy Loss** The Color Constancy Loss  $\mathcal{L}_{col}$  corrects potential color deviations by adhering to the Gray-World hypothesis [1], which assumes that the average color in a scene is achromatic. This loss ensures that the average color of the sensor channels converges towards gray and prevents potential color deviation over the entire image:

$$\mathcal{L}_{col} = \sum_{\varepsilon \in \{(R,G),(R,B),(G,B)\}} (J_p^\varepsilon - J_q^\varepsilon)^2, \quad (8)$$

where term  $J^\varepsilon$  represents the average intensity of a particular pair of color channels within the image. The indices  $p$  and  $q$  here refer to different spatial regions of the image where color constancy is being compared, and the summation runs over all combinations of the RGB channels.

**Perceptual Loss ( $\mathcal{L}_{vgg}$ ) [13]** To ensure that the enhanced image is perceptually similar to the well-lit ground truth, we employ a perceptual loss using the feature maps from a pre-trained VGG-19 network:

$$\mathcal{L}_{vgg} = \sum_{l=1}^L \frac{1}{M_l} \|\Phi_l(\hat{I}) - \Phi_l(I_{gt})\|_1 \quad (9)$$

$\Phi_l$  denotes the feature maps from the  $l^{th}$  layer of VGG-19,  $M_l$  is the number of elements in each layer,  $I_{gt}$  is the ground truth image, and  $L$  is the total number of layers used.

**Charbonnier Loss ( $\mathcal{L}_{char}$ ) [15]** Finally, we incorporate the Charbonnier loss, a smooth approximation of the L1 loss, to measure the pixel-wise difference between the enhanced image and the ground truth:

$$\mathcal{L}_{char} = \sqrt{\|\hat{I} - I_{gt}\|^2 + \epsilon^2} \quad (10)$$

where  $\epsilon$  is a small constant ensuring numerical stability. In our case, we set  $\epsilon$  as  $1e - 3$ .



**Total Loss** $\mathcal{L}_{total}$  The total loss function  $\mathcal{L}_{total}$  is a weighted combination of the Spatial Consistency Loss, Exposure Control Loss, Color Constancy Loss, VGG Loss, and Charbonnier Loss. It is computed as:

$$\mathcal{L}_{total} = \lambda_{spa} \cdot \mathcal{L}_{spa} + \lambda_{exp} \cdot \mathcal{L}_{exp} + \lambda_{col} \cdot \mathcal{L}_{col} + \lambda_{VGG} \cdot \mathcal{L}_{VGG} + \lambda_{char} \cdot \mathcal{L}_{char}, \quad (11)$$

where  $\lambda_{spa}$ ,  $\lambda_{exp}$ ,  $\lambda_{col}$ ,  $\lambda_{VGG}$ , and  $\lambda_{char}$  are the weights of the losses.

## 4 Experiment

### 4.1 Datasets and Implementation details

We evaluate our model on three paired LOL datasets. The LOL-v1, LOL-v2-real captured, and LOL-v2-synthetic, which training and testing are split into 485:15, 689:100, and 900:100. We resize the training image to the size of 224x224. We implement our framework with PyTorch on two NVIDIA 4090 GPUs with a batch size of 8. The model is trained using the AdamW optimizer with initial hyperparameters  $\beta_1 = 0.9$  and  $\beta_2 = 0.999$ . Training is conducted for 750 epochs, where the learning rate is initially set to  $1 \times 10^{-8}$  and increases to  $2 \times 10^{-5}$  over the first 75 epochs during a warmup phase. Subsequently, the learning rate is maintained at  $2 \times 10^{-5}$  until the 600th epoch, after which it follows a cosine annealing schedule down to  $1 \times 10^{-8}$  towards the end of the training at 750 epochs. The weights  $\lambda_{spa}$ ,  $\lambda_{exp}$ ,  $\lambda_{col}$ ,  $\lambda_{VGG}$ , and  $\lambda_{char}$  are set to 5, 50, 100, 0.02, and 1 respectively, to balance the scale of losses. We adopt the peak signal-to-noise ratio (PSNR) and structural similarity (SSIM) as the evaluation metrics.

methods	Flops(G)	Params(M)	LOL-v1		LOL-v2-real		LOL-v2-syn	
			PSNR	SSIM	PSNR	SSIM	PSNR	SSIM
SID [3]	13.73	7.76	14.35	0.436	13.24	0.442	15.04	0.610
Zero-DCE [8]	4.00	0.08	14.86	0.667	18.06	0.680	17.76	0.838
RF [14]	46.23	21.54	15.23	0.452	14.05	0.458	15.97	0.632
DeepLPF [18]	5.86	1.77	15.28	0.473	14.10	0.480	16.02	0.587
UFormer [20]	12.00	5.29	16.36	0.771	18.82	0.771	19.66	0.871
RetinexNet [21]	587.47	0.84	16.77	0.560	15.47	0.567	17.15	0.798
EnGAN [12]	61.01	114.35	17.48	0.650	18.23	0.617	16.57	0.734
RUAS [16]	0.83	0.003	18.23	0.720	18.37	0.723	16.55	0.652
FIDE [22]	28.51	8.62	18.27	0.665	16.85	0.678	15.20	0.612
DRBN [24]	48.61	5.27	20.15	0.830	20.29	0.831	23.22	0.927
KinD [29]	34.99	8.02	20.86	0.790	14.74	0.641	13.29	0.578
Restormer [26]	144.25	26.15	22.43	0.823	19.94	0.827	21.41	0.830
SNR-Net [23]	26.35	4.01	<b>24.61</b>	0.842	21.48	<b>0.849</b>	<b>24.14</b>	<b>0.928</b>
Retinexformer [2]	15.57	1.61	<b>25.16</b>	<b>0.845</b>	<b>22.80</b>	0.840	<b>25.67</b>	<b>0.930</b>
Ours	17.99	0.41	23.67	<b>0.876</b>	<b>24.49</b>	<b>0.895</b>	23.66	0.912

**Table 1:** Quantitative comparisons on LOL (v1 [21] and v2 [25]) datasets

## 4.2 Quantitative Results

We compare RSEND with a wide range of state-of-the-art low-light image enhancement networks. Our result significantly outperforms SOTA methods on 3 datasets while requiring much less computational and memory cost shown in Table 1.

When compared with the best CNN-based model DRBN [24], our model achieves 3.54, 4.2, and 0.44 dB improvements on LOL-v1, LOL-v2-real, and LOL-v2-synthetic datasets. Besides, our model only consumes 7.8% (0.41/5.27) parameters and 37 % (17.99/48.61) FLOPS, which is significantly smaller than many of the other high-performing models, highlighting the efficiency of our architecture. When compared with the SOTA transformer-based model Retinexformer [2], our model’s performance in LOL-v2-real dataset yields improvement for 1.69 dB while only consuming 25% (0.41/1.61) parameters FLOPS. Apart from PSNR, our model achieves SSIM scores of 0.876, 0.895, and 0.912 on each dataset, which indicates that our model not only accurately restores brightness levels but also maintains structural integrity and texture details that are crucial for perceptual quality.

## 4.3 Visual and Perceptual Comparisons

Fig. 3. shows the visual comparisons of the low-light image (left), the other model’s performance (middle), and our RSEND’s performance (right). We can see our model either makes the image lighter or detects more details, showing the effectiveness of the model in different datasets.

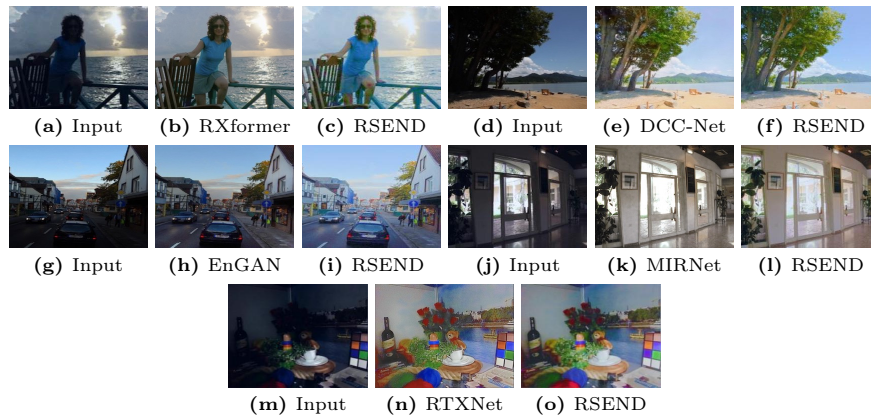


**Fig. 3:** Visual comparisons with Retinexformer [2], DC-Net [30], EnGAN [12], MIRNet [27], RetinexNet [21], our RSEND performs better

#### 4.4 Ablation Study

We perform several ablation studies to demonstrate the effectiveness of each part of our network on the LOL-v2-synthetic dataset for its stable convergence. The examples are presented in Fig. 4.

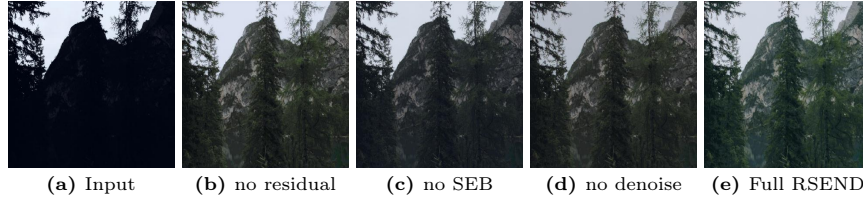


**Fig. 4:** Ablation study of the effect of each component

**Residual learning alike algorithm** We conduct an ablation to study the effectiveness of adding the original image in the end. When we just perform element-wise multiplication and denoising, our model yields 23.06 dB in PSNR and 0.902 in SSIM. However, if we add the original image after multiplication, the PSNR and SSIM values are 23.66 dB and 0.912. The difference in Fig. 4b and Fig. 4e shows that with this residual learning alike algorithm, the model achieves an improvement of 0.6 dB in PSNR and 0.01 in SSIM.

**SEBlock performance** We conduct an ablation study to evaluate the necessity of adding SEBlock. In Fig. 4c and Fig. 4e, we can clearly see the difference. The output without SEBlock is not well lighted and we can not find visually pleasing details. By adding SEBlock, the PSNR and SSIM values gain an improvement of 2.81 dB and 0.037, suggesting the necessity of using SEBlock.

**Denoise phase in the end** We conduct an ablation to study the effect of Denoising after using Retinex theory to get the final image. As we can see in Fig. 4d and Fig. 4e, even though the output without the denoising phase preserves relatively visually pleasing results, we can still find in some darker areas the details are missing. We get an improvement of 1.9 dB in PSNR and 0.02 in SSIM, which proves the layer’s efficacy in mitigating noise and preserving detail.

## 5 Conclusion

We propose an efficient and accurate CNN-based deep learning network for low-light image enhancement and it can be trained end to end with paired image. We start with Retinex theory, dividing the image into reflectance and illumination

first. In the process of enhancing, we add our illumination constraints. First, we make the model understand which parts are darker and require more attention by introducing the dark region detection module. After enhancing, we refine the output, which aims to fine-tune the details. After element-wise multiplication of reflectance and illumination, we add the original low-light image in the end, which serves as residual learning to maintain high similarity. Then we denoise the output image to ensure the final result is not only well-illuminated but also visually pleasing. For all the steps mentioned above, we utilize Squeeze and Excitation Network to better capture the details. The quantitative and qualitative experiments show that our RSEND outperforms all the CNN-based models and yields results that are close to the transformer-based models while using very few parameters.

## References

1. Buchsbaum, G.: A spatial processor model for object colour perception. *Journal of the Franklin institute* **310**(1), 1–26 (1980)
2. Cai, Y., Bian, H., Lin, J., Wang, H., Timofte, R., Zhang, Y.: Retinexformer: One-stage retinex-based transformer for low-light image enhancement. *arXiv preprint arXiv:2303.06705* (2023)
3. Chen, C., Chen, Q., Do, M.N., Koltun, V.: Seeing motion in the dark. In: *Proceedings of the IEEE/CVF International conference on computer vision*. pp. 3185–3194 (2019)
4. Coltuc, D., Bolon, P., Chassery, J.M.: Exact histogram specification. *IEEE Transactions on Image processing* **15**(5), 1143–1152 (2006)
5. Eilertsen, G., Kronander, J., Denes, G., Mantiuk, R.K., Unger, J.: Hdr image reconstruction from a single exposure using deep cnns. *ACM transactions on graphics (TOG)* **36**(6), 1–15 (2017)
6. Fan, G.D., Fan, B., Gan, M., Chen, G.Y., Chen, C.P.: Multiscale low-light image enhancement network with illumination constraint. *IEEE Transactions on Circuits and Systems for Video Technology* **32**(11), 7403–7417 (2022)
7. Farid, H.: Blind inverse gamma correction. *IEEE transactions on image processing* **10**(10), 1428–1433 (2001)
8. Guo, C., Li, C., Guo, J., Loy, C.C., Hou, J., Kwong, S., Cong, R.: Zero-reference deep curve estimation for low-light image enhancement. In: *Proceedings of the IEEE/CVF conference on computer vision and pattern recognition*. pp. 1780–1789 (2020)
9. He, K., Zhang, X., Ren, S., Sun, J.: Deep residual learning for image recognition. In: *Proceedings of the IEEE conference on computer vision and pattern recognition*. pp. 770–778 (2016)
10. Hu, J., Shen, L., Sun, G.: Squeeze-and-excitation networks. In: *Proceedings of the IEEE conference on computer vision and pattern recognition*. pp. 7132–7141 (2018)
11. Ibrahim, H., Kong, N.S.P.: Brightness preserving dynamic histogram equalization for image contrast enhancement. *IEEE Transactions on Consumer Electronics* **53**(4), 1752–1758 (2007)
12. Jiang, Y., Gong, X., Liu, D., Cheng, Y., Fang, C., Shen, X., Yang, J., Zhou, P., Wang, Z.: Enlightengan: Deep light enhancement without paired supervision. *IEEE transactions on image processing* **30**, 2340–2349 (2021)

13. Johnson, J., Alahi, A., Fei-Fei, L.: Perceptual losses for real-time style transfer and super-resolution. In: *Computer Vision–ECCV 2016: 14th European Conference, Amsterdam, The Netherlands, October 11–14, 2016, Proceedings, Part II* 14. pp. 694–711. Springer (2016)
14. Kosugi, S., Yamasaki, T.: Unpaired image enhancement featuring reinforcement-learning-controlled image editing software. In: *Proceedings of the AAAI conference on artificial intelligence*. vol. 34, pp. 11296–11303 (2020)
15. Lai, W.S., Huang, J.B., Ahuja, N., Yang, M.H.: Fast and accurate image super-resolution with deep laplacian pyramid networks. *IEEE transactions on pattern analysis and machine intelligence* **41**(11), 2599–2613 (2018)
16. Liu, R., Ma, L., Zhang, J., Fan, X., Luo, Z.: Retinex-inspired unrolling with cooperative prior architecture search for low-light image enhancement. In: *Proceedings of the IEEE/CVF Conference on Computer Vision and Pattern Recognition*. pp. 10561–10570 (2021)
17. Mantiuk, R., Daly, S., Kerofsky, L.: Display adaptive tone mapping. In: *ACM SIGGRAPH 2008 papers*, pp. 1–10 (2008)
18. Moran, S., Marza, P., McDonagh, S., Parisot, S., Slabaugh, G.: Deeplpf: Deep local parametric filters for image enhancement. In: *Proceedings of the IEEE/CVF conference on computer vision and pattern recognition*. pp. 12826–12835 (2020)
19. Ronneberger, O., Fischer, P., Brox, T.: U-net: Convolutional networks for biomedical image segmentation. In: *Medical Image Computing and Computer-Assisted Intervention–MICCAI 2015: 18th International Conference, Munich, Germany, October 5–9, 2015, Proceedings, Part III* 18. pp. 234–241. Springer (2015)
20. Wang, Z., Cun, X., Bao, J., Zhou, W., Liu, J., Li, H.: Uformer: A general u-shaped transformer for image restoration. In: *Proceedings of the IEEE/CVF conference on computer vision and pattern recognition*. pp. 17683–17693 (2022)
21. Wei, C., Wang, W., Yang, W., Liu, J.: Deep retinex decomposition for low-light enhancement. *arXiv preprint arXiv:1808.04560* (2018)
22. Xu, K., Yang, X., Yin, B., Lau, R.W.: Learning to restore low-light images via decomposition-and-enhancement. In: *Proceedings of the IEEE/CVF conference on computer vision and pattern recognition*. pp. 2281–2290 (2020)
23. Xu, X., Wang, R., Fu, C.W., Jia, J.: Snr-aware low-light image enhancement. In: *Proceedings of the IEEE/CVF conference on computer vision and pattern recognition*. pp. 17714–17724 (2022)
24. Yang, W., Wang, S., Fang, Y., Wang, Y., Liu, J.: Band representation-based semi-supervised low-light image enhancement: Bridging the gap between signal fidelity and perceptual quality. *IEEE Transactions on Image Processing* **30**, 3461–3473 (2021)
25. Yang, W., Wang, W., Huang, H., Wang, S., Liu, J.: Sparse gradient regularized deep retinex network for robust low-light image enhancement. *IEEE Transactions on Image Processing* **30**, 2072–2086 (2021)
26. Zamir, S.W., Arora, A., Khan, S., Hayat, M., Khan, F.S., Yang, M.H.: Restormer: Efficient transformer for high-resolution image restoration. In: *Proceedings of the IEEE/CVF conference on computer vision and pattern recognition*. pp. 5728–5739 (2022)
27. Zamir, S.W., Arora, A., Khan, S., Hayat, M., Khan, F.S., Yang, M.H., Shao, L.: Learning enriched features for real image restoration and enhancement. In: *Computer Vision–ECCV 2020: 16th European Conference, Glasgow, UK, August 23–28, 2020, Proceedings, Part XXV* 16. pp. 492–511. Springer (2020)

28. Zhang, K., Zuo, W., Chen, Y., Meng, D., Zhang, L.: Beyond a gaussian denoiser: Residual learning of deep cnn for image denoising. *IEEE transactions on image processing* **26**(7), 3142–3155 (2017)
29. Zhang, Y., Zhang, J., Guo, X.: Kindling the darkness: A practical low-light image enhancer. In: *Proceedings of the 27th ACM international conference on multimedia*. pp. 1632–1640 (2019)
30. Zhang, Z., Zheng, H., Hong, R., Xu, M., Yan, S., Wang, M.: Deep color consistent network for low-light image enhancement. In: *Proceedings of the IEEE/CVF conference on computer vision and pattern recognition*. pp. 1899–1908 (2022)